Journal of Catalysis 364 (2018) 394–405

Contents lists available at ScienceDirect

Journal of Catalysis

journal homepage: www.elsevier.com/locate/jcat

The first solid state porphyrin-weak acid molecular complex: A novel metal free, nanosized and porous photocatalyst for large scale aerobic oxidations in water

Akram Heydari-turkmani, Saeed Zakavi *

Department of Chemistry, Institute for Advanced Studies in Basic Sciences (IASBS), Zanjan 45137-66731, Iran

ARTICLE INFO

Article history:
Received 24 March 2018
Revised 8 June 2018
Accepted 10 June 2018

Keywords:
Photocatalysis
Porphyrin diacid
Sulfides
Sulfoxides
1,5-Dihydroxynaphthalene
Singlet oxygen
Oxidation in water

ABSTRACT

The first solid state porphyrin dication of a weak carboxylic acid was synthesized through the reaction of meso-tetrakis(N-methylpyridinium-4-yl)porphyrin (H_2TMPyP) supported on the sodium salt of Amberlyst 15 nanoparticles (nanoAmbSO_3Na) with formic acid. The polymer-porphyrin hybrid compound, nanoAmbSO_3@H_2TMPyP$(HCOOH)_2$, was characterized by FT-IR and diffuse reflectance (DR) UV–vis spectroscopy, EDX, BET, DLS, FESEM and TGA methods. Interestingly, the diacid was quite stable towards decomposition to the corresponding porphyrin and carboxylic acid in neat water as well as in acetonitrile. The protonation reaction was accompanied with the shift of the Soret band from 435 to 454 nm in DR UV–vis spectrum and a rapid color change from red brown to green. A particle size of 190 and <50 nm was estimated for the nanoparticles by DLS and FESEM, respectively. Also, the macroporous structure of the catalyst was revealed by BET experiments. nanoAmbSO_3@H_2TMPyP$(HCOOH)_2$ was used as photosensitizer for the highly chemoselective and large scale aerobic oxidation of sulfides to the corresponding sulfoxide in water within 3 h at room temperature. A conversion of ca. 95% was observed for the oxidation of sulfides to their corresponding sulfoxide in water with a selectivity of ca. 100%. The use of acetonitrile as solvent led to a significant decrease in the conversion values while retaining selectivity. The higher efficiency of the catalyst in water was in accord with greater singlet oxygen quantum yield (Φ_Δ) value of the photosensitizer in this solvent ($\Phi_\Delta = 0.41$) relative to that in acetonitrile ($\Phi_\Delta = 0.08$). Apparently, cooperative acid catalysis caused by the protic solvent and porphyrin diacid is involved in the preference of water over acetonitrile as the solvent for efficient oxidation of sulfides to sulfoxides. Furthermore, the photosensitizer was used for the efficient oxidation of 1,5-dihydroxynaphthalene (DHN) in water within 15 min. The photocatalyst was remarkably stable towards oxidative degradation so that it could be recovered and reused for at least 5 times without loss of activity. It is noteworthy that large scale photooxidation of sulfides (TON $\approx 5 \times 3000$) and DHN (TON $\approx 6 \times 1000$) were achieved in water, using nanoAmbSO_3@H_2TMPyP$(HCOOH)_2$ as the photosensitizer.

1. Introduction

Porphyrins and derivatives have been extensively used as photosensitizer in different applications such as photodynamic therapy, water treatment, medicine and biological studies [1–5]. Recently, much attention has been given to the synthesis of novel porphyrinic photosensitizers with the aim of increasing their photocatalytic activity, product selectivity and oxidative stability [6–9]. Due to the potential toxicity of most transition metals, considerable attention was paid to the synthesis of metal free catalysts [10–12]. On the other hand, owing to the high quantum yields of singlet oxygen production of metal free porphyrins as organic photosensitizers, a variety of photooxidation reactions were studied in the presence of porphyrin derivatives [13–15]. However, the recovery and reuse of catalyst has been the key challenge for using different compounds under homogeneous conditions [16]. Furthermore, the reduction of catalyst size to nanoscale is a common strategy to overcome the slow kinetics of the reaction catalyzed by heterogeneous catalysts [17–20]. On the other hand, the use of water as the most green solvent is a key component of green chemistry [21]. Porphyrin macrocycle may be substituted at the central nitrogen atoms as well as the peripheral positions [22,23]. In this regard, porphyrin core may be metallated [9], methylated [24] or protonated with different σ and π acceptors [25]. Porphyrin dications may be readily prepared by the treatment of porphyrins with

---

* Corresponding author.
E-mail address: zakavi@iasbs.ac.ir (S. Zakavi).

https://doi.org/10.1016/j.jcat.2018.06.011
0021-9517/© 2018 Elsevier Inc. All rights reserved.

different acids in organic solvents and water. The red shifted absorption bands of porphyrins diprotonated species make them interesting alternatives to the corresponding free base porphyrins [26]. However, limited attention has been devoted to developing catalyst and photocatalyst based on porphyrins diprotonated species for organic transformations [27,28]. Recently, we have reported novel porphyrin photosensitizers formed by the molecular complexation of porphyrins with 2,3-dicholoro-5,6-dicyano-1,4-benzoquinon (DDQ) and tetracyanoethylene (TCNE) [29]. The presence of DDQ and TCNE was shown to have significant effect on the photosensitizing ability of meso-tetra(aryl)porphyrins in aerobic photooxidation of olefins [25]. Also, very recently we have studied the photocatalytic activity of a series of meso-tetra(aryl) porphyrins immobilized on Amberlyst 15 nanoparticles (nanoAmb) in the form of diprotonated species [17]. In 2018, the dications of H_2TPP with different acids were used for chemoselective oxidation of sulfides to sulfoxides under homogeneous conditions [30]. In the present study, meso-tetrakis(N-methylpyridinium-4-yl)porphyrin (H_2TMPyP) was initially supported on the nano-sized anionic Amberlyst 15 formed by the alkaline treatment of this polymer. Then, the immobilized porphyrin was protonated with formic acid to prepare the core protonated porphyrin (Fig. 1). To our knowledge, it is the first report on the synthesis and characterization of a porphyrin dication with a weak carboxylic acid. Interestingly, the dication was completely stable in different solvents and water. Our previous studies [13] showed that the dications of soluble porphyrins with formic acid are readily decomposed to the corresponding free base porphyrins upon dilution in organic solvents or exposure to water. Also, the dications cannot be dried under vacuum or air flow. This observation gives evidence for remarkable impact of porphyrin immobilization on the stability of porphyrin diacid with weak acids. Furthermore, the solid compound is stable under light conditions and may be stored for a long time. It is noteworthy that due to the low acid strength of formic acid ($pK_a = 3.75$) [31], the acid cannot reprotonate the neutralized Amberlyst 15 bed ($pK_a = -6.5$) [32]. Moreover, the major weakness of formic acid prevents its involvement in unexpected side reactions. The nano-sized catalyst was used for the aerobic photooxidation of sulfides in neat water as the solvent. The selective oxidation of sulfides to the corresponding sulfoxide is still a challenging synthetic problem that may be achieved through singlet oxygen mediated photooxidation of sulfides under mild conditions [33–35]. Herein, acid catalysis [36–38] induced by the porphyrin diacid and the protic solvent is also involved in the observed rate of the photooxidation reactions. It is noteworthy that sulfoxides are important intermediates in organic synthesis pharmaceutical industry [39,40]. Furthermore, the catalytic activity of the immobilized porphyrin diacid in the oxidation of 1,5-dihydroxynaphthalene (DHN) was investigated [41]. The product of oxidation or photooxidation of DHN, i.e. 5-hydroxy-1,4-naphthoquinone (Juglone) is a naturally occurring aromatic compound which plays an important role in the pharmaceutical and dye industries [42–44]. On the other hand, oxidative degradation of DHN is of importance for the removal of phenolic and naphtholic pollutants from wastewater [45]. The main objective of this study is to present the effects of weak carboxylic acids on the photocatalytic activity and oxidative stability of porphyrins in photooxidation of organic substrates in water under heterogeneous conditions.

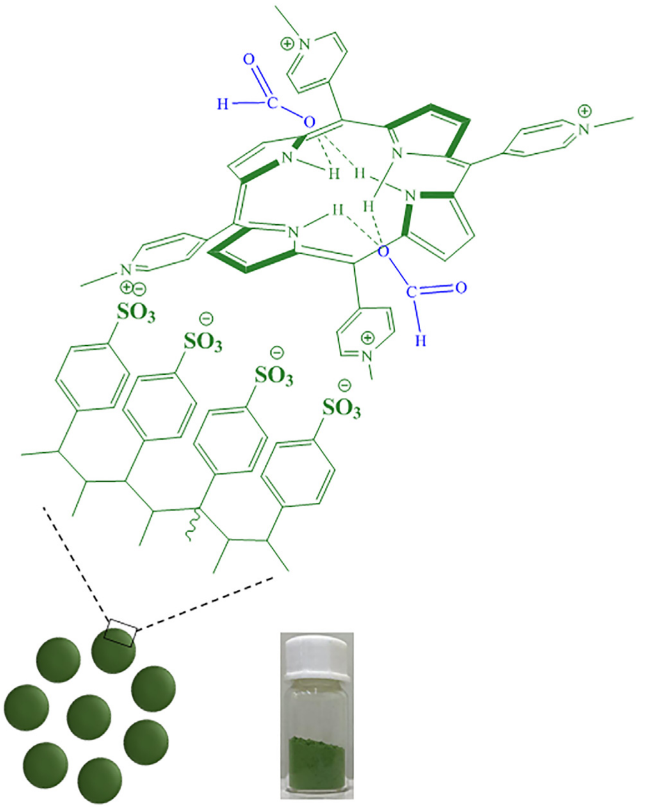

Fig. 1. Immobilization of H_2TMPyP on nanoAmbSO_3Na and its protonation with formic acid.

2. Experimental

2.1. Instrumental

A Pharmacia Biotech Ultrospec 4000 UV–vis spectrophotometer and a Varian Cary 5000 UV–Vis–NIR absorption spectrometer were used for preparation of UV–vis and diffuse reflectance UV–vis spectra, respectively. ^{1}H NMR spectra were obtained on a Bruker Avance DPX-400 MHz spectrometer. The reaction mixtures were analyzed using a Varian-3800 gas chromatograph with a HP-5 capillary column and flame-ionization detector. FT-IR spectra were prepared using a Bruker Vector 22 instrument. A Belsorp max (Japan) instrument was employed for porosimetry analyses using the nitrogen adsorption/desorption method. The mean diameter and size distribution of the solid catalyst before and after loading of porphyrin were measured by Zetasizer Nano ZS (Malvern Instruments Ltd, United Kingdom) at 25 °C with a detection angle of 90°. For morphology characterization by FE-SEM, the crushed Amberlyst beads obtained after 24 h were placed on a clean glass slide and then vacuum-coated with gold. Digital images of the samples were taken with HitachiS4160 field emission scanning electron microscope operating at 20 kV.

2.2. Amberlyst 15 nanoparticles (nanoAmb)

Amberlyst 15 beads (dry, ion-exchange resin, ACROS) were stirred vigorously over a magnetic stirrer in ethyl acetate overnight at room temperature to obtain the pale yellow powder of nanoAmb. Details of nanoparticle characterization were described elsewhere [17].

2.3. Preparation of porphyrins

Meso-tetra(4-pyridyl)porphyrin (H_2TPyP) and 5,10,15,20-tetrakis(N-methylpyridinium-4-yl)porphyrin tetra(p-toluenesulfonate), H_2TMPyP, were prepared and purified according to the literature methods [46]. The UV–vis and ^{1}H NMR spectral data of the used porphyrin are as follows:

$H_2T(4\text{-}Py)P$: ^1H NMR ($CDCl_3$, 400 MHz): δ -2.93 (2H, br, s, NH), 8.15–8.17 ($8H_m$, dd), 9.06–9.07 ($8H_o$, dd), 7.90 (4H, m), 8.87 ($8H_\beta$, s); UV–Vis (λ/nm) in CH_2Cl_2: 418 (Soret), 512, 547, 588, 646.

H_2TMPyP: ^1H NMR (DMSO d_6, 400 MHz): −2.81 (2H, br, s, NH), 3.84 (12H, $-CH_3$), 9.27–9.28 ($8H_o$, d), 9.48 ($8H_\beta$, s), 9.77–9.79 ($8H_m$, m) (see Supplementary material, S1 for the ^1H NMR spectrum of the counteranion, p-toluenesulfonate), UV–Vis (λ/nm) in water: 420 (Soret), 515, 553, 582, 635.

2.4. Immobilization of $H_2TMPyP(HCOOH)_2$ on $nanoAmbSO_3Na$

The sodium salt of nanoAmb was prepared by treatment of Amberlyst 15 (1.5 g in 30 ml distilled water) with a 1 M sodium hydroxide solution. The mixture was stirred magnetically for 24 h. After the required time, the solid was centrifugally separated. The precipitate was thoroughly washed by distilled water in a centrifuge tube until neutral and finally dried in a vacuum desiccator (24 h). To prepare the immobilized porphyrin, an excess amount of H_2TMPyP was added to $nanoAmbSO_3Na$ in water. The mixture was magnetically stirred for 5 h in dark and then the solid was separated by centrifuge (5000 rpm). The solid residue was washed by centrifuge with distilled water thoroughly until a colourless aqueous phase was observed. The remaining solutions were analyzed by UV–vis spectroscopy to measure the non-immobilized porphyrin; a calibration curve (absorbance vs. concentration) obtained for H_2TMPyP in water was used to determine the non-supported porphyrin. A maximum loading of 0.076 g H_2TMPyP per one gram of $nanoAmbSO_3$ corresponding to a loading of 0.052 mmol g^{-1} was measured. In a previous study [17], we have shown that a low loading of porphyrin (0.003 mmol of porphyrin per 1 g of the polymer, 0.003 mmol g^{-1}) is more efficient in aerobic photooxidation of olefins. Indeed, the maximum conversion of olefin to the oxidation product was observed under this loading condition. Accordingly, in the present study, we have examined different catalyst loadings and a catalyst loading of 0.007 mmol g^{-1} (0.010 g of H_2TMPyP per 1 g of the polymer) was found to be the optimum one. It is noteworthy that upon the addition of an amount of H_2TMPyP less than the maximum capacity of $nanoAmbSO_3Na$, no non-immobilized porphyrin remained in the solution after the centrifuge separation of the solid residue.

Then, the immobilized porphyrin was protonated with an excess amount of formic acid (beyond 1:2 M ratio of porphyrin to acid) to prepare the core protonated porphyrin for 2 h. The immobilization of porphyrin on the polymer was confirmed by diffuse reflectance UV–vis and IR spectroscopy.

2.5. General oxidation procedure

Photooxidation of sulfides and DHN was performed in a double walled cylindrical glass vessel (Supplementary material, S2). Water was circulated through the outer jacket to maintain a constant temperature. In a typical reaction photosensitizer (6.6×10^{-4} mmol, 0.094 g) and sulfide (2 mmol) were added to 10 ml of the desired solvent (acetonitrile, water or water/acetonitrile in 1:1 ratio) to obtain the 1:3000 M ratio of the catalyst to substrate. At different time intervals, an aliquot of the solution was taken out with a syringe and analyzed by GC. In the case of DHN, the catalyst (0.0003 mmol) and substrate (0.003 mmol) were used. The progress of the oxidation of DHN was monitored by UV–vis spectroscopy; the oxidation of DHN was accompanied with the decrease in the intensity of the absorption band at 301 nm ($\varepsilon = 7664\ M^{-1}\ cm^{-1}$) and the increase of the band at 415 nm ($\varepsilon = 3811\ M^{-1}\ cm^{-1}$). A 10 W white LED lamp was used as the light source for the oxidation of DHN. In the case of sulfides, different lamps (20 W blue, red and white LED lamps and sunlight were used as the light source). In order to characterize the products of the oxidation of sulfides, at different time intervals (Fig. 9) the reaction mixture was extracted with ethyl acetate, rotary evaporated, dissolved in $CDCl_3$ and analyzed by ^1H NMR and ^{13}C NMR. The NMR spectra confirmed the formation of sulfoxide as nearly the exclusive product.

1-(methylsulfinyl)benzene: Methyl(phenyl)sulfane (248 mg, 2 mmol) was oxidized according to the above general oxidation procedure using $nanoAmbSO_3@H_2TMPyP(HCOOH)_2$ (0.66×10^{-3} mmol). Crude material was separated by Thin-layer chromatography (TLC) (1:4 ratio of ethyl acetate, n-hexane) to give methyl phenyl sulfoxide; yield: (91%). ^1H NMR (400 MHz, chloroform-d): $\delta = 7.56–7.38$ (m, 5H), 2.61 (s, 3H). ^{13}C NMR (400 MHz, chloroform-*d*): $\delta = 43.57$ ppm ($-CH_3$), 145.22 (–CS–), 123.26 (C_o), 129.27 (C_m), 130.79 (C_p). (Supplementary material, S3 (a,b)).

1-(ethylsulfinyl)-4-methylbenzene: Ethyl(p-tolyl)sulfane (292.6 mg, 2 mmol) was performed according to the general procedure using $nanoAmbSO_3@H_2TMPyP(HCOOH)_2$ (0.66×10^{-3} mmol). Crude material was separated by TLC (1:4 ratio of ethyl acetate, n-hexane) to give Ethyl phenyl sulfoxide; yield: (90%). ^1H NMR (400 MHz, chloroform-d): $\delta = 7.60–7.45$ (m, 4H), 2.91–2.82 (m, 1H), 2.77–2.68 (m, 1H), 1.15 (t, 3H). ^{13}C NMR (400 MHz, chloroform-*d*): $\delta = 5.65$ ppm (CH_3CH_2-), 21.35 (CH_3Ph-), 49.73 (-CH_2S-), 142.89 (-CS-), 128.87 (C_p), 123.78 (C_o), 130.90 (C_m) (Supplementary material, S4 (a,b)).

1-methoxy-4-(methylsulfinyl)benzene: (4-methoxyphenyl)(methyl)sulfane (308.4 mg, 2 mmol) was performed according to the general procedure using $nanoAmbSO_3@H_2TMPyP(HCOOH)_2$ (0.66×10^{-3} mmol). Crude material was separated by TLC (1:4 ratio of ethyl acetate, *n*-hexane) to give Methoxy phenyl sulfoxide; yield: 95%. ^1H NMR (400 MHz, chloroform-d): $\delta = 7.42$ (d, 2H), 6.85 (d, 2H), 3.65 (s, 3H), 2.51 (s, 3H). ^{13}C NMR (400 MHz, chloroform-*d*): $\delta = 161.18$ (-CS-), 136.41(C_p)., 125.59 (C_m), 114.87 (C_o)., 55.37 (CH_3S-), 43.60 (OCH_3Ph-) (Supplementary material, S5 (a,b)).

1-chloro-4-(methylsulfinyl)benzene: (4-Chlorophenyl)(methyl)sulfane (317.2 mg, 2 mmol) was performed according to the general procedure using $nanoAmbSO_3@H_2TMPyP(HCOOH)_2$ (0.66×10^{-3} mmol). Crude material was separated by TLC (1:4 ratio of ethyl acetate, n-hexane) to give 4-chlorophenyl phenyl sulfoxide; yield: (90%). ^1H NMR (400 MHz, chloroform-d): $\delta = 7.57–7.55$ (m, 2H), 7.47–7.45 (m, 2H), 2.69 (s, 3H). ^{13}C NMR (400 MHz, chloroform-*d*): $\delta = 144.29$ (-CS-) ppm, 136.91 (C_p), 129.65 (C_m), 124.90 (C_o), 43.84 (CH_3Ph-), (Supplementary material, S6 (a,b)).

1-(butylsulfinyl)butane: Dibutylsulfane (292.6 mg, 2 mmol) was performed according to the general procedure using $nanoAmbSO_3@H_2TMPyP(HCOOH)_2$ (0.66×10^{-3} mmol). Crude material was separated by TLC (1:4 ratio of ethyl acetate, n-hexane) to give dibutyl sulfoxide; yield: (80%). ^1H NMR (400 MHz, chloroform-d): $\delta = 2.72–2.59$ (m, 4H), 1.78–1.70 (m, 4H), 1.55–1.40 (m, 4H), 0.97 (t, 6H). ^{13}C NMR (400 MHz, chloroform-*d*): $\delta = 52.09$ (-CS-) ppm, 24.89 (-CH2-), 22.10 (-CH_2CH_3), 13.71 (-CH_3) (Supplementary material, S7 (a,b)).

2.6. Singlet oxygen quantum yield determination

The Φ_Δ value of the photosensitizer was measured through the reaction of the reactive oxygen species (ROS) with 1,3-diphenylisobenzofuran (DPBF) as a quencher of singlet oxygen and methylene blue ($\Phi_\Delta = 0.52$ in water and acetonitrile) [47] as a reference photosensitizer. The equation $\Phi_\Delta = \Phi_\Delta^{std} \times (\upsilon_i \times I^{std}/\upsilon_i^{std} \times I)$ proposed by Murata et al. was used to determine the Φ_Δ value. In this equation, Φ_Δ^{std}, υ_i, υ_i^{std}, I^{std} and I present the Φ_Δ of methylene blue, the rate of DPBF (8×10^{-4} M) oxidation in the presence of the photosensitizer and a 10 W red LED lamp, the rate of DPBF oxidation in the presence of methylene blue, the number of photons absorbed by the standard solution and those absorbed by the photosensitizer, respectively [48].

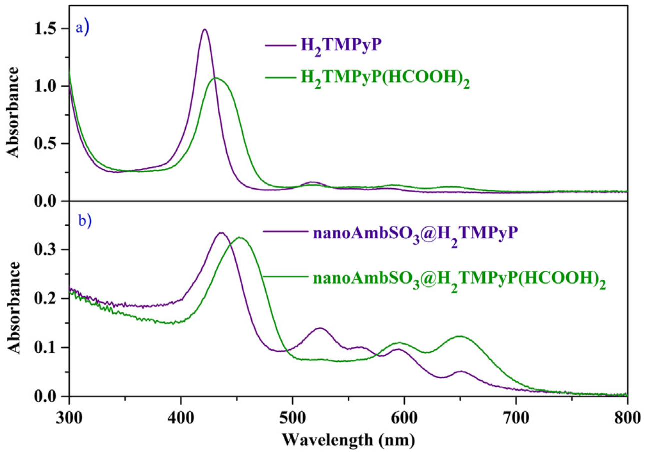

Fig. 2. (a) UV–vis spectra of H_2TMPyP and the corresponding dication with formic acid in water. (b) Diffuse reflectance UV–vis spectra of H_2TMPyP immobilized on $nanoAmbSO_3Na$ and its formic acid dication.

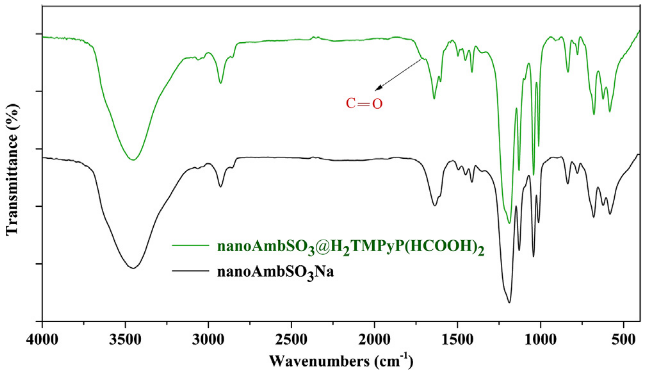

Fig. 3. FT-IR spectra of $nanoAmbSO_3@H_2TMPyP$ and $nanoAmbSO_3@H_2TMPyP(HCOOH)_2$ (KBr disk).

3. Results and discussion

3.1. Immobilization of porphyrin

The cationic porphyrin H_2TMPyP was supported on the anionic polymer by electrostatic interactions. The diffuse reflectance UV–vis spectrum of $nanoAmbSO_3@H_2TMPyP$ is shown in (Fig. 2).

The Soret and Q bands of the immobilized porphyrin appeared at 435, 525, 558, 595 and 650 nm. The addition of formic acid to the immobilized porphyrin led to change in the colour of the solid from grey to green; diffuse reflectance UV–vis spectra of the green solid (Fig. 2b, green curve) is in accord with the formation of porphyrin diacid. Fig. 2a (purple curve) demonstrates the UV–vis of H_2TMPyP in water with the Soret and Q bands at 420, 525, nm. As seen in Fig. 2b (green curve), the Soret and Q bands of H_2TMPyP shift to longer wavelengths through protonation of porphyrin core with HCOOH. Accordingly, the DR-UV–vis spectrum clearly shows the immobilization of porphyrin on the polymer in the form of porphyrin diacid. Furthermore, the comparison of the IR spectra of $nanoAmbSO_3@H_2TMPyP$ and $nanoAmbSO_3@H_2TMPyP(HCOOH)_2$ (Fig. 3) shows the appearance of a band at 1750 cm^{-1} that is attributed to the presence of formic acid in the polymer structure.

Energy-dispersive X-ray spectroscopy (EDS) analyses and elemental mapping were performed on $nanoAmbSO_3Na$, $nanoAmbSO_3@H_2TMPyP$ and $nanoAmbSO_3@H_2TMPyP(HCOOH)_2$ (Fig. 4). The results shown in Supplementary material, S8 demonstrate uniform distribution of different elements on the solid compound.

Also, the elemental analyses based on EDX measurements is in accord with the formation of the respective compounds; the molar ratio of oxygen to sulfur significantly increased from $nanoAmbSO_3Na$ to $nanoAmbSO_3@H_2TMPyP(HCOOH)_2$. It is noteworthy that due to the possible different hydrophilicity of $nanoAmbSO_3Na$, $nanoAmbeSO_3@H_2TMPyP$ and $nanoAmbSO_3@H_2TMPyP(HCOOH)_2$ there are some differences between the amounts of water absorbed by these compounds.

3.2. DLS and SEM of nanostructures

The formation of $nanoAmbSO_3Na$ and $nanoAmbSO_3@H_2TMPyP(HCOOH)_2$ was confirmed by dynamic light scattering (DLS) and

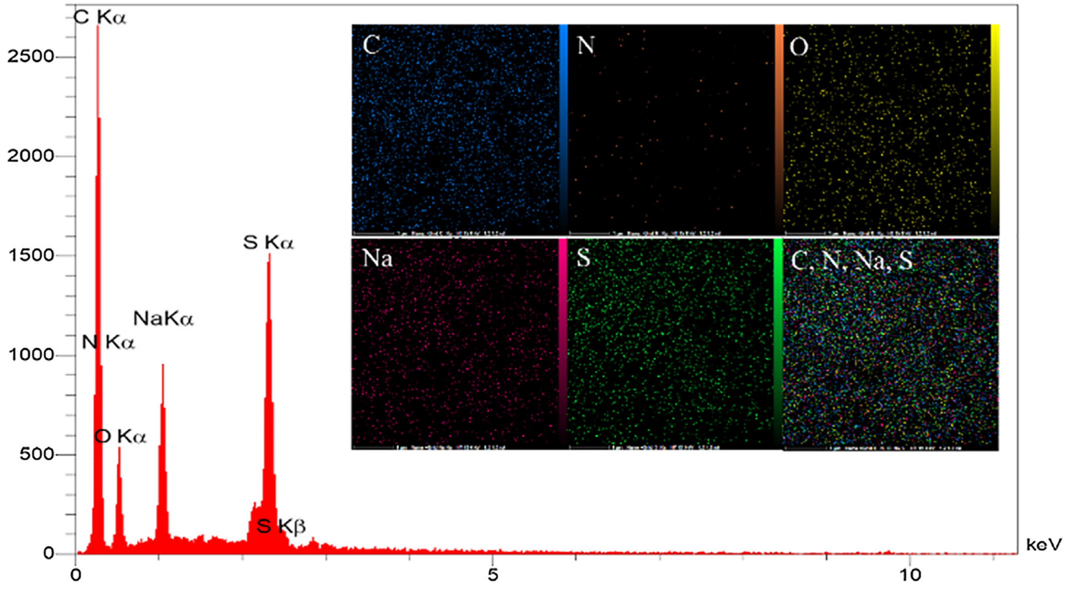

Fig. 4. EDS pattern and carbon, nitrogen, oxygen, sodium and sulfur elemental mapping captured for $nanoAmbSO_3@H_2TMPyP(HCOOH)_2$.

Field-emission scanning electron microscopy (FESEM). As was explained elsewhere [17], the polymer nanoparticles were prepared by magnetically stirring overnight Amberlyst 15 beads in water. In the present work, the acidic polymer was magnetically stirred in a 1 M solution of NaOH. DLS measurements show a particle size of 191 and 189.9 nm for nanoAmbSO$_3$Na and nanoAmbSO$_3$@H$_2$TMPyP(HCOOH)$_2$, respectively with a homogeneous size distribution. Accordingly, the immobilization of porphyrin and the formation of porphyrin diacid had little or no effects on the size of the polymer nanostructures. On the other hand, FESEM images indicate a significantly smaller size (<50 nm) for nanoAmbSO$_3$@H$_2$TMPyP(HCOOH)$_2$ (Fig. 5).

The nitrogen sorption isotherms of the solid catalysts (Fig. 6) are in accord with the macroporous structure of the catalyst. Also, significant decrease in BET pore volume (V_{total}) and surface area (S_{BET}) values was observed after the immobilization and protonation of the porphyrin (Table 1). Thermal gravimetry analysis (TGA) of nanoAmbSO$_3$Na, nanoAmbSO$_3$@H$_2$TMPyP and nanoAmbSO$_3$@H$_2$TMPyP(HCOOH)$_2$ are shown in (Fig. 7). The changes below ca. 100 °C show dehydration or other small molecule loss. As seen from Fig. 7 and Supplementary material, S9, the weight loss in this region is more pronounced in the case of nanoAmbSO$_3$Na and nanoAmbSO$_3$@H$_2$TMPyP. This observation seems to be due to the larger amount of the adsorbed water molecules in these structures compared to that of nanoAmbSO$_3$@H$_2$TMPyP(HCOOH)$_2$. TGA curves display the major weight-loss stage above 450 °C. In the case of the three compounds the weight loss occurs at ca. 450 °C. Also, comparable weight losses are observed for nanoAmbSO$_3$@H$_2$TMPyP(HCOOH)$_2$, nanoAmbSO$_3$Na and nanoAmbSO$_3$@H$_2$TMPyP. Accordingly, the protonation of porphyrin core had little effect on the thermal stability of the immobilized porphyrin.

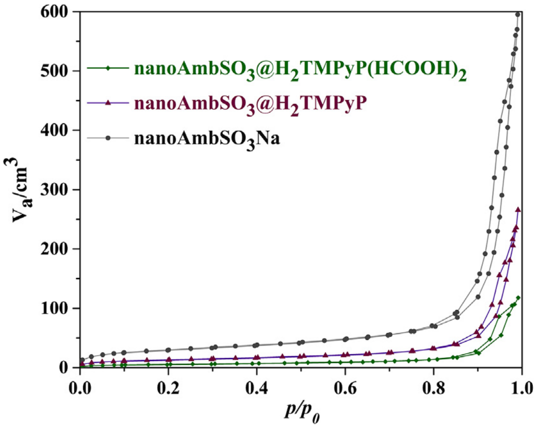

Fig. 6. N$_2$ adsorption/desorption isotherms of nanoAmbSO$_3$Na and the immobilized porphyrin.

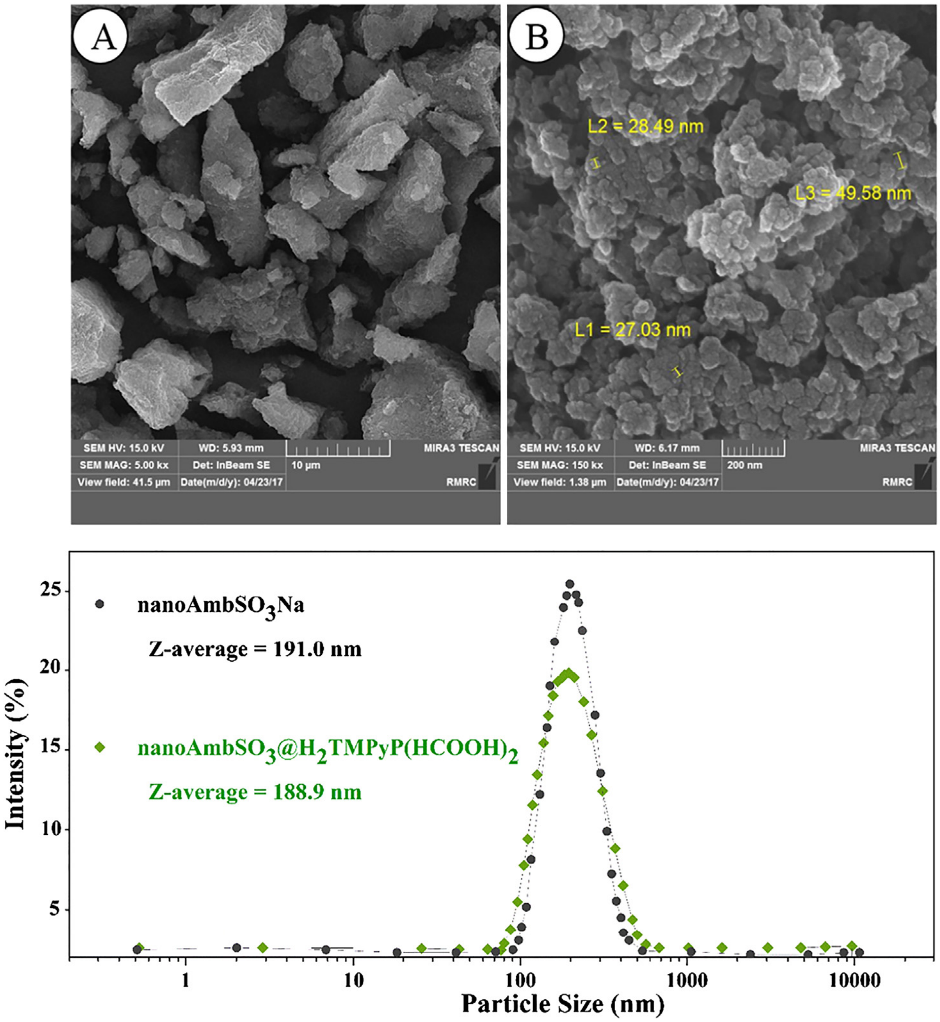

Fig. 5. FE-SEM (A and B) and DLS characterization of nanoAmbSO$_3$Na and nanoAmbSO$_3$@H$_2$TMPyP(HCOOH)$_2$.

Table 1
BET analysis of $nanoAmbSO_3Na$ and the immobilized catalyst.

Photosensitizer	S_{BET}[a] ($m^2\ g^{-1}$)	V_t ($cm^3\ g^{-1}$)[b]
$nanoAmbSO_3Na$	107	0.914
$nanoAmbSO_3@H_2TMPyP$	47	0.401
$nanoAmbSO_3@H_2TMPyP(HCOOH)_2$	20	0.179

[a] S_{BET} is the specific surface area.
[b] V_t is the total pore volume.

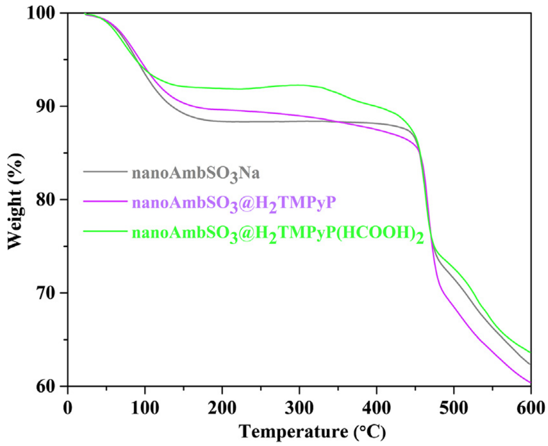

Fig. 7. TGA of $nanoAmbSO_3Na$, $nanoAmbSO_3@H_2TMPyP$ and $nanoAmbSO_3@H_2TMPyP(HCOOH)_2$ under nitrogen atmosphere at a heating rate of 10 K/min.

3.3. Photooxidation of alkyl aryl sulfides

$NanoAmbSO_3@H_2TMPyP(HCOOH)_2$ has the potential to be used as a red shifted heterogeneous photocatalyst for the oxidation of organic compounds. In order to elucidate the influence of protonation on the photocatalytic performance of $nanoAmbSO_3@H_2TMPyP$, the oxidation of methyl phenyl sulfide was conducted in the presence of $nanoAmbSO_3Na$, $nanoAmbSO_3@H_2TMPyP$ and the formic acid protonated counterpart (Table 2) under different reaction conditions (Scheme 1).

As seen from Table 2, the use of $nanoAmbSO_3@H_2TMPyP$ led to the formation of sulfoxides and sulfone in ca. 2:1 M ratio (sulfoxide selectivity = 67%). Under the same conditions, conducting the reaction in the presence of $nanoAmbSO_3@H_2TMPyP(HCOOH)_2$ gave sulfoxide as the nearly exclusive product. This observation seems to be due to the stabilization of the persulfoxide intermediate by hydrogen bond formation with porphyrin diacid (*vide infra*) [48]. It is noteworthy that the lack of such hydrogen bonds leads to the formation of a cyclic persulfoxide through the nucleophilic attack of the peroxide residue on the sulfur atom of the persulfoxide intermediate. The migration of oxygen atom following this step leads to the formation of sulfone as the product. Furthermore, stabilization of the sulfoxide product caused by hydrogen bond formation with hydrogen bond donors such as porphyrin diacid prevents further oxidation of sulfoxide to sulfone [49]. The steric hindrance due to the hydrogen bond donors attached to the sulfoxide product was also proposed to be involved in the increased sulfoxide selectivity [50]. In accord with these observations, conducting the oxidation of methyl phenyl sulfide in water led to a significantly increased conversion values and reaction rates. In other words, cooperative acid catalysis caused by the protic solvent and porphyrin diacid is involved in the preference of water over acetonitrile as the solvent for efficient oxidation of sulfides to sulfoxides. It should be noted that the small size of water molecule makes it a more efficient hydrogen bond donor than porphyrin diacid. The oxidation of methyl phenyl sulfide was also studied in the presence of $nanoAmbSO_3@H_2TMPyP$ in water (entry 9). Herein, methyl phenyl sulfoxide obtained as the sole product, but the catalyst was subject to extensive oxidative degradation under the reaction conditions. In a control experiment, ethanol was added to the reaction mixture (entry 10) and a ca. 10% increase in the conversion value was observed. This observation seems to be due to the increased solubility of methyl phenyl sulfide in water caused by dissolved ethanol. On the other hand, ethanol is expected to be a better hydrogen bond donor [51] and therefore a stronger acid catalyst than the former. This in turn would increase the rate of photooxidation reaction (*vide infra*).

3.4. Catalyst to substrate optimum molar ratio

The immobilized catalyst was employed for the oxidation of sulfides. In a very recent paper [30] it was shown that under homogeneous conditions, the free base porphyrin has a decreased photocatalytic activity and photooxidative stability compared to those of the corresponding dication. Also, the reaction time for a conversion of 48% was 24 h that was much longer than that in the case of the

Table 2
Effect of catalyst to substrate molar ratio and solvent on the oxidation of methyl phenyl sulfide.[a]

Entry	Catalyst	Catalyst:sulfide molar ratio	Solvent	Time	Conversion[b] (%) Sulfoxide (Sulfone)	Selectivity(%)	TON[c](TOF, h^{-1})[d]
1	$nanoAmbSO_3Na$	0:1000	CH_3CN	3 h	N.R	N.R	N.R
2	$nanoAmbSO_3@H_2TMPyP$	1:1000	CH_3CN	3 h	25 (12)	67	370 (123)
3	$nanoAmbSO_3@H_2TMPyP(HCOOH)_2$	1:1000	CH_3CN	3 h	32 (<1)	~100	320 (106)
4	$nanoAmbSO_3@H_2TMPyP(HCOOH)_2$	1:1000	H_2O	1 h	49 (<1)	~100	490 (490)
5	$nanoAmbSO_3@H_2TMPyP(HCOOH)_2$	1:1000	H_2O	2 h	91 (<1)	~100	910 (455)
6	$nanoAmbSO_3@H_2TMPyP(HCOOH)_2$	1:1000	H_2O	3 h	97 (<1)	~100	970 (323)
7	$nanoAmbSO_3@H_2TMPyP(HCOOH)_2$	1:2000	H_2O	2 h	60 (<1)	~100	1200 (600)
8	$nanoAmbSO_3@H_2TMPyP(HCOOH)_2$	1:3000	H_2O	2 h	65 (<1)	~100	1950 (975)
9	$nanoAmbSO_3@H_2TMPyP$[e]	1:3000	H_2O	2 h	44 (<1)	~100	1320 (660)
10	$nanoAmbSO_3@H_2TMPyP$[f,g]	1:3000	H_2O	2 h	55 (<1)	~100	1650 (825)
11	$nanoAmbSO_3@H_2TMPyP(HCOOH)_2$	1:3000	$H_2O:CH_3N$	3 h	45 (<1)	~100	1350 (450)
12	$nanoAmbSO_3@H_2TMPyP(HCOOH)_2$	1:3000	H_2O	3 h	91 (<1)	~100	2730 (910)

[a] A 20 W white LED lamp was used as the light source.
[b] All reactions were repeated three times, analyzed by GC and the average values were reported. The formation of sulfoxide as the main product was also confirmed by ^1H NMR (Fig. 9).
[c] TON demonstrates the number of moles of the product obtained per one mole of the catalyst.
[d] TOF shows the turnover number of the reaction per time unit.
[e] An oxidative degradation of ca. 50% was observed for the catalyst at the end of the first run.
[f] For the photooxidation reaction performed in the presence of ethanol; catalyst and alcohol was used in 1:1 M ratio.
[g] An oxidative degradation of ca. 70% was observed for the catalyst.

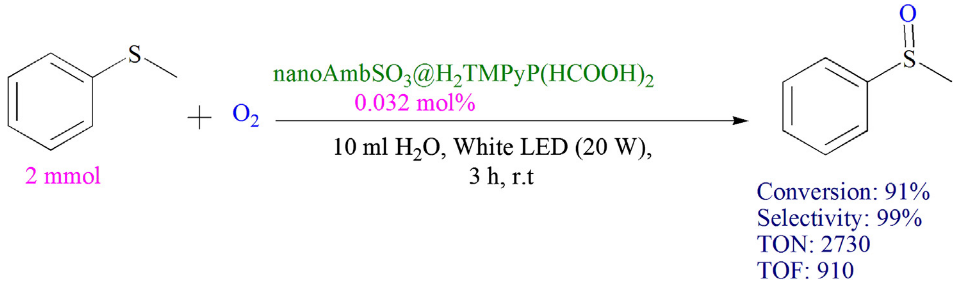

Scheme1. The optimized conditions for aerobic sulfoxidation of methyl phenyl catalyzed by nanoAmbSO_3@H_2TMPyP$(HCOOH)_2$.

dication. It was shown that the protonation of porphyrin core leads to a remarkable increase in the photocatalytic activity and oxidative stability of the porphyrin photosensitizer.

Previous studies showed that the catalyst to substrate molar ratio and solvent play crucial roles in the efficiency of the photooxidation reactions conducted in the presence of porphyrinic photosensitizers. In order to study the effects of these parameters, the oxidation of methyl phenyl sulfide was performed under different conditions (Table 2 and Fig. 8). As seen from Table 2, the use of water as solvent led a significant increase in the conversion value in comparison with that achieved in acetonitrile with no effect on product selectivity. Indeed, very little sulfone product was obtained for reaction times less than 3 h. Also, the use of 1:1 mixture of water and acetonitrile caused a two times increase in the conversion (Table 2, entry 11). The oxidation reaction was also studied using catalyst and methyl phenyl sulfide in 1:1000 to 1:5000 M ratios. Although the maximum conversion was observed in the case of the 1:1000 ratio, the use of 1:3000 M ratio led to much higher turnover number (TON) and frequencies (TOF) of the reaction. Accordingly, the 1:3000 M ratio (entry 12) and a reaction time of 3 h were used as the optimum reaction conditions. It is noteworthy that no catalyst degradation or leaching was observed within a reaction time of 3 h. In order to find the effects of the reaction time on the product selectivity, the oxidation of methyl phenyl sulfide was also conducted for a reaction time of 6 h.

The oxidation of different sulfides was studied to find the influence of the groups attached to sulfur atom (Table 3). It is observed that the presence of Cl and OCH_3 group at the phenyl group has little or no effect on the reactivity of sulfide. It should be noted that $-OCH_3$ is an efficient electron-releasing group to phenyl ring and in electrophilic substitution of benzene ring is an activating group directing to the ortho/para positions.

However, the absence of aryl group at the sulfur atom led to a decrease in the reactivity of the sulfur atom. In the case of dibutyl sulfide, sulfone was also obtained that was attributed to the acid character of the aliphatic CH protons the formation of persulfoxide led to an increase in the acidity of the CH bonds adjacent to the SOO^- group of the persulfoxide [38,49] (Table 3, entry 5). This in turn leads to an increase in the electron density at the carbon atom adjacent to the sulfur atom and consequently leads to increased reactivity of the sulfur group towards overoxidation to the corresponding sulfone compound. The reaction was also performed using air as the oxygen source (Table 4) and a decrease in the rate of the oxidation reaction was observed; the reaction time for nearly complete conversion of methyl phenyl sulfide to the corresponding sulfoxide increased from 3 to 5 h.

It is noteworthy that the use of air as the molecular oxygen source lowers the cost of the overall process and is in line with the green chemistry principles. The risk of ignition will be considerably increased by even a few percent oxygen enrichment of the atmosphere [52]. As was expected, no reaction was observed in under nitrogen atmosphere.

The immobilized catalyst may be recycled and reused at least 5 times without any detectable loss in the catalytic activity. Furthermore, no catalyst degradation or leaching was observed in a time interval of 3–5 h. The degree of degradation of the porphyrinic catalyst was only ca. 40% after the fifth cycle (Fig. 10 and Supplementary material, S10).

3.5. Effect of the light source

The oxidation of methyl phenyl sulfide was performed using different light sources (see Supplementary material, S11 for the

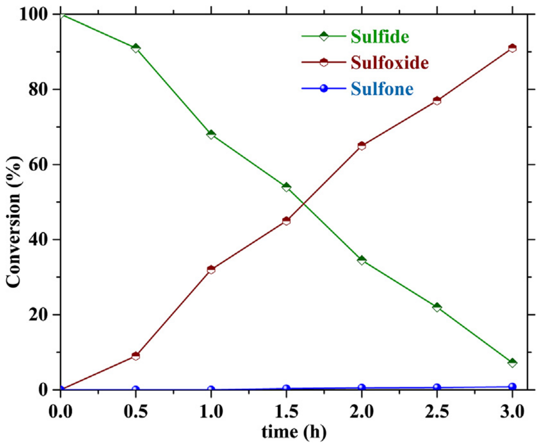

Fig. 8. The formation of methyl phenyl sulfoxide as the main product upon the oxidation of methyl phenyl sulfide.

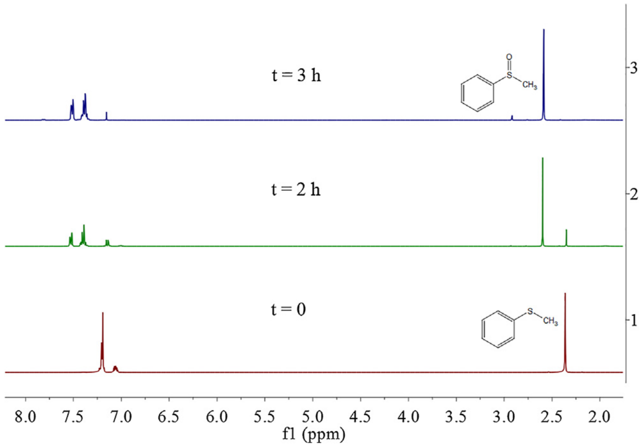

Fig. 9. ^1H NMR spectrum of the reaction mixture in $CDCl_3$ at different time intervals; after the required time, the organic phase was extracted with ethyl acetate, dried with rotary evaporator and dissolved in $CDCl_3$.

Table 3
Photooxidation of different Sulfides.[a]

Entry	Substrate	Product	Conversion[b] [Selectivity] (%)	Photostability (%)	TON	TOF (h^{-1})
1	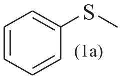 (1a)	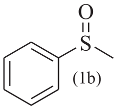 (1b)	91 [100]	>95	2730	910
2	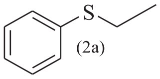 (2a)	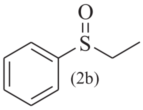 (2b)	90 [100]	>95	2700	900
3	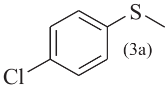 (3a)	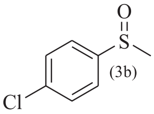 (3b)	90 [100]	>95	2700	900
4	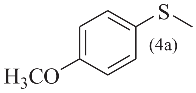 (4a)	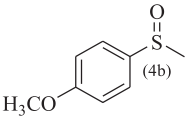 (4b)	95 [100]	>95	2850	950
5	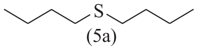 (5a)	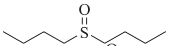 (5b) 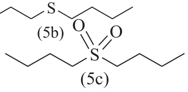 (5c)	80 [90] 15 [10]	>95	2400	800

[a] Catalyst and sulfides were used in a 1:3000 M ratio in water.
[b] GC yield; all products were characterized by ^{1}H NMR and ^{13}C NMR (Supplementary material, S3–S7).

Table 4
Photocatalytic oxidation of methyl phenyl sulfide under nitrogen, air and oxygen atomosphere.[a]

Atmosphere	Time	Conversion [Sulfoxide selectivity] (%)	TON (TOF, h^{-1})
O_2	3 h	91 [100]	2730 (910)
Air	3 h	47 [100]	1410 (470)
Air	5 h	93 [100]	2790 (465)
N_2	3 h	Trace	–

[a] See the footnotes of Tables 2 and 3 for more details.

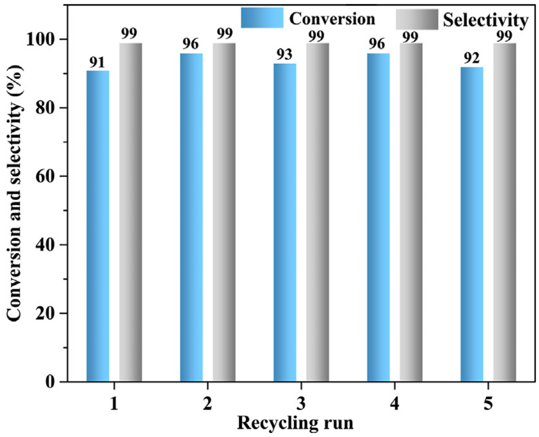

Fig. 10. Reusability of nanoAmbSO$_3$@H$_2$TMPyP(HCOOH)$_2$ under the optimized reaction conditions.

Table 5
Effect of light source on the photooxidation of methyl phenyl sulfide under the optimum conditions.[a]

Light source	Conversion (%)	Selectivity (%)	TON [TOF (h^{-1})]
White LED (20 W)	91	100	2730 [910]
Blue LED (20 W)	46	100	1380 [460]
Red LED (20 W)	20	100	600 (200)
Sunlight	88	100	2640 (880)

[a] See the footnotes of Tables 2 and 3 for more details.

emission spectra of the light sources) and under Sunlight irradiation (Table 5). It is observed that in spite of large changes in the conversion value, the selectivity of the reaction towards sulfoxide was completely independent of the light source. The higher efficiency of the blue LED lamps versus the red LED one is in accord with the higher intensity of the absorption band of porphyrin diacid in the Soret band region. However, there is no large difference between the conversion values achieved in the presence if the blue and red LED lamps. The latter shows that the excitation at the Soret and Q bands region are both involved in the photosensitizing process.

3.6. Proposed mechanism

The oxidation of organic substrates in the presence of porphyrinic photosensitizers may proceed through a singlet oxygen mediated or charge transfer mechanism [53]. Control experiments (Supplementary material, S12a) confirm that no reaction occurs in the absence of the photocatalyst. The oxidation of sulfides usually occurs by the intermediacy of a persulfoxide species (Scheme 2) [49]. The increased sulfoxides selectivity in the presence of porphyrin diacid in comparison with that observed in the case of the immobilized free base porphyrin is probably due to the acid catalysis by porphyrin diacid. Furthermore, the significantly higher conversion value in water compared to that in acetonitrile seems to be due to the hydrogen bond stabilized persulfoxide intermediate as well as the increased singlet oxygen quantum yield of the photosensitizer in water relative to that in acetonitrile (*vide infra*); herein, porphyrin diacid and water cooperatively stabilize the intermediate and direct the reaction towards the formation of persulfoxide as the sole product. The addition of furfuryl alcohol as a

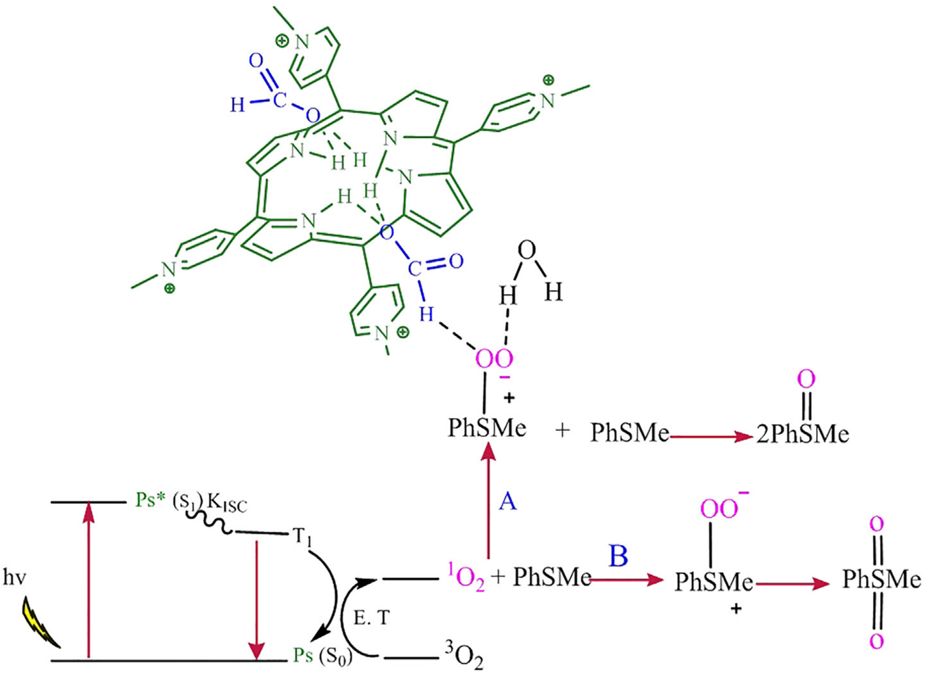

Scheme 2. Proposed mechanism for photooxidation of sulfides; (A) acid catalysis by porphyrin diacid and water; (B) sulfone formation.

singlet oxygen quencher led to a significant decrease in the conversion of methyl phenyl sulfide to the oxidation product [54]. Also, the irradiation of catalyst with a red LED lamp in presence of 1,3-diphenylisobenzofuran (DPBF) in water led to fast decay of the band due to DPBF at ca. 420 nm (Fig. 11). It is noteworthy that the later is a well-known singlet oxygen quencher [55,56]. However, a conversion of 6% was achieved under this condition. On the other hand, running the oxidation reaction in the presence of 1,4-benzoquinone as a scavenger of superoxide anion radical led to a ca. 7% decrease in the conversion (Supplementary material, S12b). Accordingly, singlet oxygen is proposed to be the key reactive intermediate in this catalytic system. However, the formation of superoxide anion radical is also involved as the minor reaction pathway. Furthermore, hot filtration test of the reaction mixture (Fig. 12) showed that the oxidation reaction was terminated completely by catalyst removal. Also, the results confirmed the absence of catalyst leaching during the oxidation reaction.

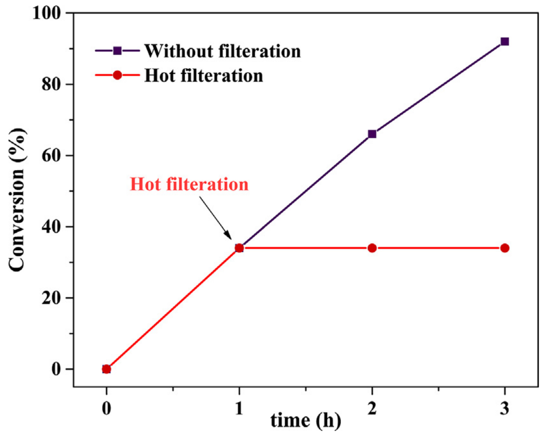

Fig. 12. The effect of removal of the catalyst (hot filtration) after 1 h on the progress of the oxidation reaction.

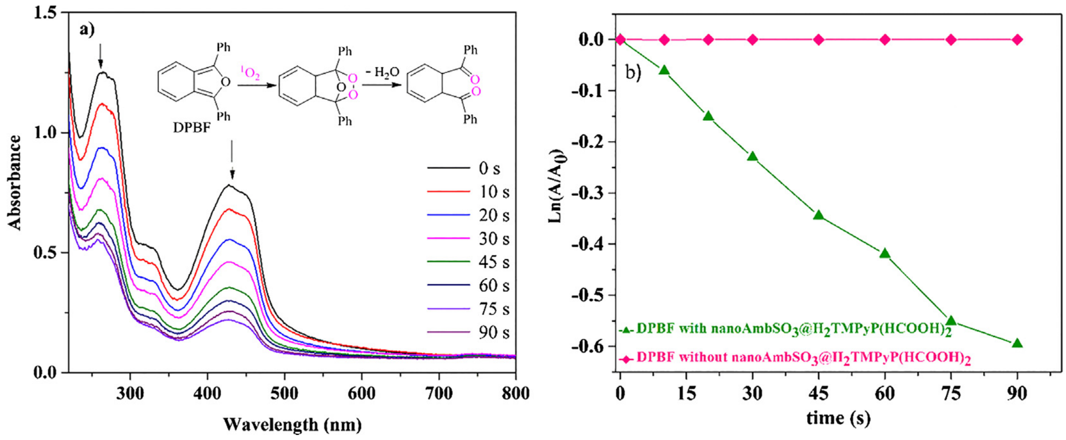

Fig. 11. The change in the UV–vis spectrum of DPBF (a) in the presence of nanoAmbSO$_3$@H$_2$TMPyP(HCOOH)$_2$ in water using a 10 W red LED lamp as the light source. Fig. b shows the changes at the λ_{max} of DPBF vs. time.

3.7. Singlet oxygen quantum yield

The singlet oxygen quantum yield (Φ_Δ) of photosensitizers, a quantitative measurement of the efficiency of photosensitizers to use the absorbed light to convert triplet molecular oxygen into singlet oxygen ($^1\Delta_g$) species, is as an important parameter to evaluate the efficiency of novel photocatalysts [57]. The Φ_Δ value of nanoAmbSO$_3$@H$_2$TMPyP(HCOOH)$_2$ was measured by using DPBF as the quencher of singlet oxygen and methylene blue ($\Phi_\Delta = 0.52$ in water and acetonitrile) [47] as a reference photosensitizer. The experimental details and equations used for the measurement of Φ_Δ value were described elsewhere [58]. The Kinetics curves used for the Φ_Δ measurements and the changes in the absorption spectrum of DPBF in the presence of the photosensitizers in water and acetonitrile are shown in Fig. 13d; a ca. 5 fold increase in the observed rate constant of BPBF photooxidation is observed from acetonitrile to water. In spite of the fact that singlet oxygen has a much shorter lifetime in water (2 μs) in comparison with that in most organic solvents (30, 69 and 75 μs in acetonitrile, toluene and dichloromethane, respectively) [59,60], a Φ_Δ value of 0.41 was measured in water that is significantly greater than that in neat acetonitrile ($\Phi_\Delta = 0.08$) which correlates with higher efficiency of the photosensitizer in water (Table 2). The increased Φ_Δ value of the polymer supported porphyrin in water seems to be due to the polymer swelling in water caused by the hydrophilicity of Amb [61] which makes the immobilized porphyrin more accessible to triplet oxygen. Furthermore, polymer swelling can facilitate the entrance and exit of oxygen molecules into and out of the polymer phase. It is noteworthy that the formation of singlet oxygen necessitates the entrance of triplet oxygen into the porphyrin sites bounded to the polymeric matrix. On the other hand, the exit of singlet oxygen from the polymeric matrix prevents the quenching of singlet oxygen before reaction with DPBF used for the measurement of Φ_Δ value.

3.8. Oxidation of 1,5-dihydroxynaphthalene

Oxidation of DHN to Juglone was studied in acetonitrile, water and a 1:1 mixture of water and acetonitrile (Fig. 14, Table 6 and Supplementary material, S13). As seen from Table 6, the oxidation reaction completed in 15 min in water as solvent. The use of the 1:1 ratio of acetonitrile and water increased the reaction time to 45 min. Also, conducting the oxidation reaction in neat acetonitrile led to a remarkable decreased in the rate of the reaction. Again, the higher efficiency of the photooxidation reaction is in accord with higher Φ_Δ value in water compared to that in acetonitrile. As was observed in the case of sulfides, the use of water instead of acetonitrile led to a remarkable decrease in the reaction rate from 180 to 15 min. The oxidation of DHN to Juglone was suggested to occur through a hydroperoxide intermediate (Scheme 3) [43,62,63]. Accordingly, the hydrogen bond formation ability of water which stabilizes the hydroperoxide intermediate seems to be also involved in higher conversion values observed in water.

Furthermore, previous studies revealed the increased reaction rates under weak acidic conditions [62]. It is noteworthy that the presence of porphyrin diacid as the photosensitizer leads to weak acid conditions in this catalytic system.

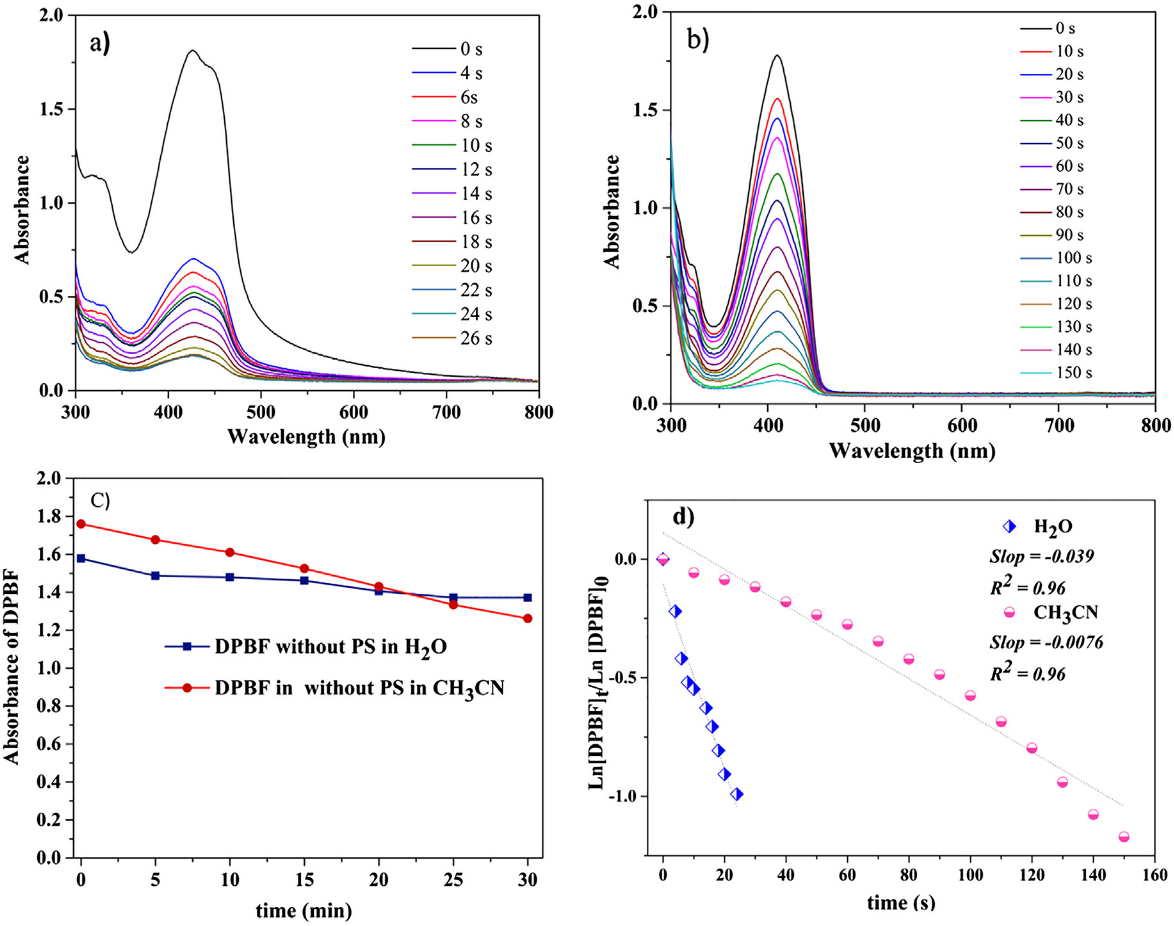

Fig. 13. The change in the UV–vis spectrum of DPBF upon irradiation with a 10 W red LED lamp in the presence of nanoAmbSO$_3$@H$_2$TMPyP(HCOOH)$_2$ in water (a) and acetonitrile (b). C and d show the rate of DPBF photooxidation in water and acetonitrile, respectively.

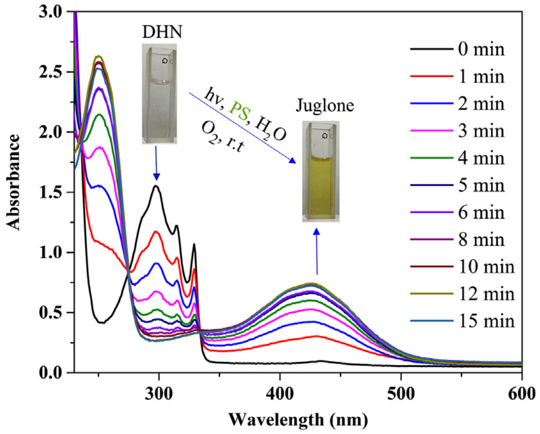

Fig. 14. Photooxidation of DHN in water catalyzed by nanoAmbSO$_3$@H$_2$TMPyP (HCOOH)$_2$ as the photosensitizer (PS). The formation of Juglone as the product was also confirmed by ^{1}H NMR (Supplementary material, S14).

Table 6
Photooxidation of DHN.[a,b]

Entry	Solvent	Time (min)	Φ_Δ	k_{obs}[c] (s^{-1})	Yield[d] (%)
1	CH_3CN	180	0.08	0.0076	84
2	CH_3CN: H_2O	45	–	–	98
3	H_2O	15	0.41	0.039	98
4	H_2O	90[e]	0.41	0.039	98

[a] Catalyst (0.0003 mmol) and DHN (0.003 mmol) were used in 1:10 M ratio.
[b] A white LED lamp (10 W) was used as the light source.
[c] The observed rate constants for the oxidation of DPBF (Fig. 13d).
[d] On the basis of the absorption change at the λ_{max} (427 nm, ε = 3811 cm^{-1} M^{-1}) of the product.
[e] Large scale conditions using 0.0003 mmol catalyst and 0.3 mmol DHN.

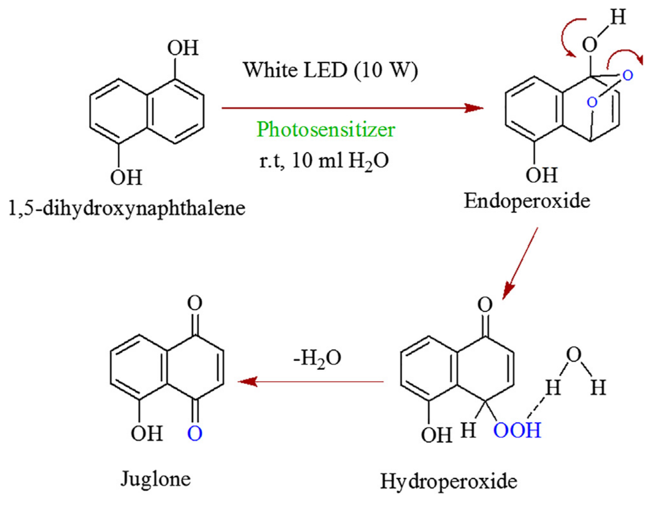

Scheme 3. Oxidation of DHN to Juglone. Hydrogen bond formation between the hydroperoxide intermediate of DHN and water in addition to the intramolecular hydrogen bond are probably involved in the stabilization of the intermediate.

4. Conclusion

In this study, H_2TMPyP was immobilized on nanostructured Amberlyst 15 sodium salt to form nanoAmbSO$_3$@H$_2$TMPyP. The immobilized porphyrin was protonated with formic acid in water to give nanoAmbSO$_3$@H$_2$TMPyP(HCOOH)$_2$ with significantly red shifted Soret and Q bands. To our knowledge, it is the first report on a thoroughly stable porphyrin dication with a weak carboxylic acid in solid state. Furthermore, in contrast to the dication of porphyrins with weak acids, the immobilized porphyrin diacid was highly stable toward decomposition to the fragments upon exposure to different solvents including acetonitrile, ethyl acetate, water and acetonitrile/water mixed solvent. NanoAmbSO$_3$@H$_2$-TMPyP(HCOOH)$_2$ was used as a novel photosensitizer for large scale aerobic photooxidation of sulfides and DHN under heterogeneous conditions in water, acetonitrile and water/acetonitrile at room temperature. The remarkable increase in the efficiency of nanoAmbSO$_3$@H$_2$TMPyP(HCOOH)$_2$ for the oxidation of sulfides in water is probably due to the ability of the protic solvent and protonated porphyrin to stabilize the persulfoxide intermediate through hydrogen bond formation with the persulfoxide intermediate. Furthermore, water induced swelling of the polymer support may be also involved in the increased catalytic performance of the catalyst. Interestingly, the immobilized porphyrin diacid showed a remarkable oxidative stability under reaction conditions. Also, it was recovered and reused at least 5 times in the oxidation of sulfides to achieve complete and highly selective oxidation of the organic substrates to their corresponding sulfoxide within 3 h. It is noteworthy that a maximum porphyrin degradation of ca. 40% was observed after the fifth cycle. On the other hand, the oxidation of DHN completed within a reaction time of 15 min in water. Running the oxidation of sulfides in the presence of furfurylalcohol and 1,4-benzoquinone showed the involvement of singlet oxygen and superoxide anion radical as the major and minor reactive oxidant species, respectively.

Acknowledgements

Financial Support of this work by the Institute for Advanced Studies in Basic Sciences (IASBS) is gratefully acknowledged.

Appendix A. Supplementary material

Supplementary data to this article can be found online at https://doi.org/10.1016/j.jcat.2018.06.011.

References

[1] M. Ethirajan, Y. Chen, P. Joshi, R.K. Pandey, Chem. Soc. Rev. 40 (2011) 340–362.
[2] Z. Luksiene, P. Juzenas, J. Moan, Cancer Lett. 235 (2006) 40–47.
[3] S.L.H. Rebelo, M. Linhares, M.M.Q. Simões, A.M.S. Silva, M.G.P.M.S. Neves, J.A.S. Cavaleiro, C. Freire, J. Catal. 315 (2014) 33–40.
[4] G. Mele, R.D. Sole, G. eVasapollo, E. Garcıa-López, L. Palmisano, M. Schiavello, J. Catal. 217 (2003) 334–342.
[5] J. Zhao, W. Wu, J. Sun, S. Guo, Chem. Soc. Rev. 42 (2013) 5323–5351.
[6] S.M. Ribeiro, A.C. Serra, A.M.d'A. Rocha Gonsalves, J. Catal. 256 (2008) 331–337.
[7] A.A. Ghogare, A. Greer, Chem. Rev. 116 (2016) 9994–10034.
[8] J. Yeow, S. Shanmugam, N. Corrigan, R.P. Kuchel, J. Xu, C. Boyer, Macromolecules 49 (2016) 7277–7285.
[9] M. Hajimohammadi, N. Safari, H. Mofakham, F. Deyhimi, Green Chem. 13 (2011) 991–997.
[10] M.-Q. Yang, N. Zhang, Y. Wang, Y.-J. Xu, J. Catal. 346 (2017) 21–29.
[11] M.J. Lima, A.M.T. Silva, C.G. Silva, J.L. Faria, J. Catal. 353 (2017) 44–53.
[12] P. Zhang, Y. Wang, H. Li, M. Antonietti, Green Chem. 14 (2012) 1904–1908.
[13] S. Zakavi, S. Hoseini, A.G. Mojarrad, New J. Chem. 41 (1059) (2017) 11053–11061.
[14] D. Murtinho, M. Pineiro, M.M. Pereira, A.M.d.A.R. Gonsalves, L.G. Arnaut, M. da Graça Miguel, H.D. Burrows, J. Chem. Soc. Perkin Trans. 2 (2000) 2441–2447.
[15] X.-F. Liu, R.-X. Li, X.-T. Ren, Y.-B. Yin, S.-K. Mei, T. Liu, J. Yan, J. Catal. 348 (2017) 314–320.
[16] A.D. Vylder, J. Lauwaert, D. Esquivel, D. Poelman, J.D. Clercq, P.V.D. Voort, J.W. Thybaut, J. Catal. 361 (2018) 51–61.
[17] A. Heydari-turkmani, S. Zakavi, N. Nikfarjam, New J. Chem. 41 (2017) 5012–5020.
[18] Y. Zhi, K. Li, H. Xia, M. Xue, Y. Mu, X. Liu, J. Mater. Chem. A 5 (2017) 8697–8704.
[19] J. Zhang, Z. Zhang, B. Yu, C. Wang, W. Wu, X. Jiang, ACS Appl. Mater. Interfaces 8 (2016) 5794–5803.
[20] J. Liu, G. Liu, C. Liu, W. Li, F. Wang, Catal. Sci. Technol. 6 (2016) 2055–2059.
[21] P.T. Anastas, J.C. Warner, Green Chemistry: Theory and Practice, Oxford University Press, 2000.

[22] D. Mohajer, H. Dehghani, J. Chem. Soc. Perkin Trans. 2 (2000) 199–205.
[23] D. Mohajer, S. Zakavi, S. Rayati, M. Zahedi, N. Safari, H.R. Khavasi, S. Shabazian, New J. Chem. 27 (2003) 242–244.
[24] M. Roucan, M. Kielmann, S. Connon, S. Bernhard, M. Senge, Chem. Commun. 54 (2018) 26–29.
[25] A.G. Mojarrad, S. Zakavi, RSC Adv. 6 (2016) 100931–100938.
[26] Z. Amara, J.F. Bellamy, R. Horvath, S.J. Miller, A. Beeby, A. Burgard, K. Rossen, M. Poliakoff, M.W. George, Nat. Chem. 7 (2015) 489–495.
[27] S. Zakavi, G.R. Karimipour, N. Gholami Gharab, Catal. Commun. 10 (2009) 388–390.
[28] S. Frühbeißer, G. Mariani, F. Gröhn, Polymers 8 (2016) 180–198.
[29] A.G. Mojarrad, S. Zakavi, Eur. J. Inorg. Chem. (2017) 2854–2862.
[30] A.G. Mojarrad, S. Zakavi, Catal. Sci. Technol. 8 (2018) 768–781.
[31] S. Zakavi, N.G. Gharab, Polyhedron 26 (2007) 2425–2432.
[32] Y. Chang, C. Lee, C. Bae, RSC Adv. 4 (2014) 47448–47454.
[33] T. Neveselý, E. Svobodová, J. Chudoba, M. Sikorski, R. Cibulka, Adv. Synth. Catal. 358 (2016) 1654–1663.
[34] X. Gu, X. Li, Y. Chai, Q. Yang, P. Li, Y. Yao, Green Chem. 15 (2013) 357–361.
[35] T. Uematsu, Y. Miyamoto, Y. Ogasawara, K. Suzuki, K. Yamaguchi, N. Mizuno, Catal. Sci. Technol. 6 (2016) 222–233.
[36] C. Xing, J. Deng, R. Tan, M. Gao, P. Hao, D. Yin, D. Yin, Catal. Sci. Technol. 7 (2017) 5944–5952.
[37] T. Akasaka, M. Haranaka, W. Ando, J. Am. Chem. Soc. 113 (1991) 9898–9900.
[38] S.M. Bonesi, A. Albini, J. Org. Chem. 65 (2000) 4532–4536.
[39] M.C. Carreño, Chem. Rev. 95 (1995) 1717–1760.
[40] S. Caron, R.W. Dugger, S.G. Ruggeri, J.A. Ragan, D.H.B. Ripin, Chem. Rev. 106 (2006) 2943–2989.
[41] J. Zhu, G. Sun, J. Mater. Chem. 22 (2012) 10581–10588.
[42] S. Zakavi, S. Hoseini, ChemistrySelect 1 (2016) 5008–5013.
[43] E.E. Coyle, K. Joyce, K. Nolan, M. Oelgemöller, Green Chem. 12 (2010) 1544–1547.
[44] J. Sun, J. Zhao, H. Guo, W. Wu, Chem. Commun. 48 (2012) 4169–4171.
[45] K. Mondal, S. Bhattacharyya, A. Sharma, Ind. Eng. Chem. Res. 53 (2014) 18900–18909.
[46] K. Kalyanasundaram, Inorg. Chem. 23 (1984) 2453–2459.
[47] F. Wilkinson, W.P. Helman, A.B. Ross, J. Phys. Chem. Ref. Data 22 (1993) 113–262.
[48] S.y. Takizawa, R. Aboshi, S. Murata, Photochem. Photobiol. Sci. 10 (2011) 895–903.
[49] E.L. Clennan, Acc. Chem. Res. 34 (2001) 875–884.
[50] S. Zakavi, A. Abasi, A.R. Pourali, S. Talebzadeh, Bull. Kor. Chem. Soc. 33 (2012) 35–38.
[51] M. Heger, T. Schargez, M.A. Suhm, Phys. Chem. Chem. Phys. 15 (2013) 16065–16073.
[52] T. Abbasi, S. Abbasi, J. Hazard. Mater. 140 (2007) 7–44.
[53] M.C. DeRosa, R.J. Crutchley, Coord. Chem. Rev. 233 (2002) 351–371.
[54] E. Appiani, R. Ossola, D.E. Latch, P.R. Erickson, K. McNeill, Environ. Sci. Process. Impact 19 (2017) 507–516.
[55] J. Park, D. Feng, S. Yuan, H.C. Zhou, Angew. Chem. Int. Ed. 127 (2015) 440–445.
[56] E. Gürel, M. Pişkin, S. Altun, Z. Odabaş, M. Durmuş, Dalton Trans. 44 (2015) 6202–6211.
[57] P. Majumdar, X. Yuan, S. Li, B. Le Guennic, J. Ma, C. Zhang, D. Jacquemin, J. Zhao, J. Mater. Chem. B 2 (2014) 2838–2854.
[58] P. Kubát, P. Henke, V. Berzediová, M. Stepanek, K. Lang, J. Mosinger, ACS Appl. Mater. Interfaces 9 (2017) 36229–36238.
[59] P.B. Merkel, d.D.R. Kearns, J. Am. Chem. Soc. 94 (1972) 7244–7253.
[60] C.A. Long, D.R. Kearns, J. Am. Chem. Soc. 97 (1975) 2018–2020.
[61] Z. Wang, H. Liu, H. Cui, M. Zhang, Z. Zhang, Ind. Eng. Chem. Res. 54 (2015) 7219–7225.
[62] J.H. Cai, J.-W. Huang, P. Zhao, Y.-H. Zhou, H.-C. Yu, L.-N. Ji, J. Mol. Catal. A Chem. 292 (2008) 49–53.
[63] K.T. de Oliveira, L.Z. Miller, D.T. McQuade, RSC Adv. 6 (2016) 12717–12725.